STUDY OF CAVITY IMPERFECTION IMPACT ON RF-PARAMETERS AND MULTIPOLE COMPONENTS IN A SUPERCONDUCTING RF-DIPOLE CAVITY*

R. G. Olave, J. R. Delayen†, S. U. De Silva, Old Dominion University, Norfolk, VA, USA
Z. Li, SLAC National Accelerator Laboratory, Menlo Park, CA, USA

Abstract

The ODU/SLAC superconducting rf-dipole cavity is under consideration for the crab-crossing system in the upcoming LHC luminosity upgrade. While the proposed cavity complies well within the rf-parameters and multipolar component restrictions for the LHC system, cavity imperfections arising from cavity fabrication, welding and frequency tuning may have a significant effect in these parameters. We report on an initial study of the impact of deviation from the ideal shape on the cavity's performance in terms of rf-parameters and multipolar components.

INTRODUCTION

Due to transverse geometry constraints at the nominal operating rf frequency of 400 MHz, novel compact cavities are under consideration for the upcoming LHC High Luminosity upgrade. The ODU/SLAC superconducting rf-dipole cavity is a suitable candidate as it satisfies the requirements for high gradients, high shunt impedance, low surface fields, no lower order modes, and well-defined and widely-spaced higher order modes [1]-[3]. The cavity geometry, while compact, is not azimuthally symmetric and therefore it becomes important to identify any higher order multipolar components at the operating frequency, since these can lead to beam instabilities in the LHC system. The ODU/SLAC rf-dipole cavity satisfies all specifications for the LHC crab cavity system in terms of rf parameters and in terms of multipole contributions up to the octupole term [4]; Table 1 presents a list of the relevant rf parameters for the cavity. As we prepare for fabrication of a prototype cavity, we are analyzing the impact of individual imperfections or departures from the ideal cavity geometry, that may arise from fabrication or welding errors, while additional distortions would result from the tuning process. In this paper, we present an initial analysis on how such geometry imperfections, particularly those due to welding of the poles, would result in the introduction of undesired higher order multipole components.

IMPERFECTIONS IN THE POLES VS FIELD UNIFORMITY

The design optimization of the cavity showed quite clearly that the geometry of the aperture region of the poles

---

Table 1: RF Parameters of the 400 MHz Rf-dipole Cavity (at $E_T = 1$ MV/m and Reference Length $\beta_0\lambda$)

Parameter		Units
Frequency	400.28	MHz
$(R/Q)_T$	412.7	Ω
$(R/Q)_T * (QR_s)$	4.43x10^4	Ω^2
E_p/E_T	3.66	
B_p/E_T	6.14	mT (MV/m)

near the beam axis is of vital importance in minimizing the contribution of the sextupole component, which results in a more uniform deflecting voltage across the beam aperture region. For this reason, we start by looking into imperfections in the shape or welding of the poles. Using CST Microwave Studio® 2012 (CST MWS) we have altered the optimized design near the beamline to introduce individual defects in the alignment or geometry of one of the poles, according to the following list:

- (A) Yaw (rotation about y-axis) of one pole.
- (B) Pitch (rotation about x-axis) of one pole.
- (C) Roll (rotation about z-axis) of one pole.
- (D) Horizontal displacement of one pole.
- (E) Vertical displacement of one pole.
- (F) Blending radius at the outer corner of one pole.
- (G) Blending radius of the feather-like structure near the beamline of one pole.
- (H) Aperture radius in one pole.

Figure 1 shows transverse and longitudinal views of the cavity, where the optimized pole geometry can clearly be seen, as well as the places where deformations have been added according to the previous list.

The robustness of the cavity design is such that none of the individual imperfections introduced so far produces drastic changes in the rf-parameters. For items (A), (F) and (G), the transverse voltages (normalized to the transverse voltage at the ideal cavity's beamline) barely change as function of transverse offset from the ideal beamline, from those of the ideal cavity geometry. This can be seen for example in Fig. 2, which includes a plots for different yaw (rotation about the y-axis) angles, as well as a plot (red) of the transverse voltage as a function of transverse offset of the ideal cavity for reference. As can be seen, there is field uniformity in a large region within the cavity's aperture, even for large yaw angles in one of the poles.
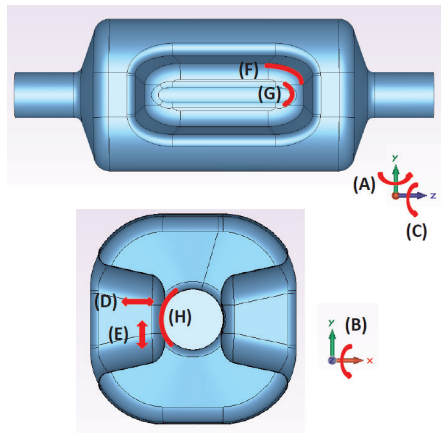
Figure 1: Longitudinal and transverse views of the optimized cavity, and individual imperfections that have been introduced in the geometry of the left pole.
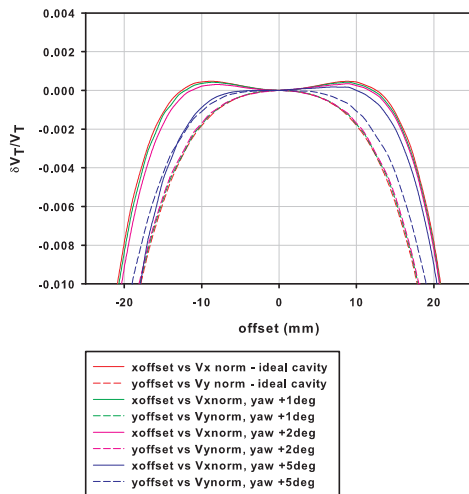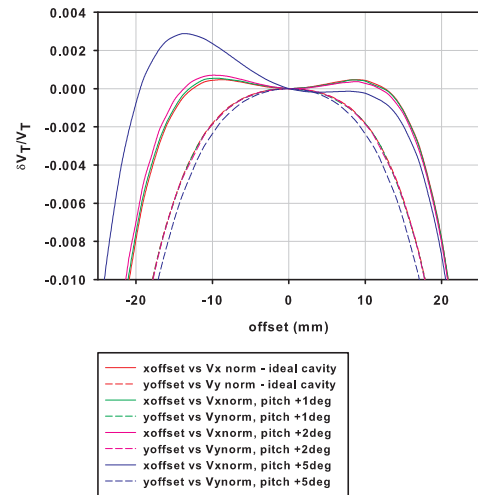

Figure 3: Effects of the pitch (rotation about the x-axis) of one pole on the normalized transverse voltages.

It is worthwhile to note that even for large imperfections, such as a roll angle of 5°, the change in the normalized transverse voltages is on the order of a few percent.
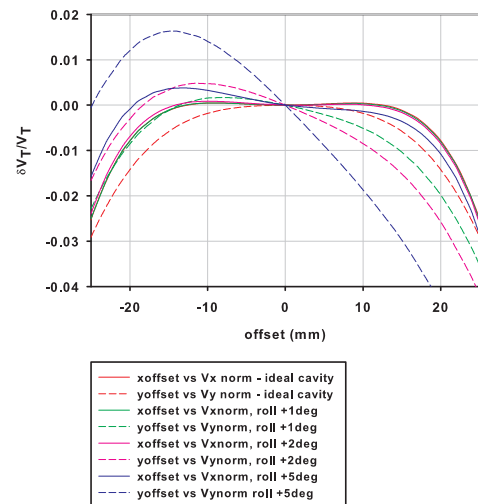

Figure 2: Effects of the yaw (rotation about the y-axis) of one pole on the normalized transverse voltages in the aperture region.

Figure 4: Effects of the roll (rotation about the z-axis) of one pole on the transverse voltages.

The introduction of a pitch angle results in changes similar to those of displacing a pole in the vertical direction, items (B) and (E). These result in an asymmetry in the horizontal (x-direction) voltage profile, accompanied by displacement of the electrical center of the cavity. This can clearly be seen in Fig. 3, which shows the effects of the pitch (rotation about the x-axis) of one of the poles on the normalized transverse voltage as a function of transverse offset.

The largest effects on the normalized transverse voltages seen so far are due to the roll (rotation about the z-axis) of one of the poles. These effects can be seen in Fig. 4 as a sharp asymmetry in the vertical (y-axis) voltage profile, as well as a displacement on the electrical center of the cavity.

The effect of a horizontal displacement of one of the poles, item (D), is simply to shift the electrical center of the cavity. The effects of changing the aperture radius of one of the poles, item (H), is still under analysis.

IMPERFECTIONS OF THE POLES VS MULTIPOLE COMPONENTS

Following the procedure outlined in [5]-[8], from the interpolation of the electromagnetic fields on the surface of a virtual cylinder of radius R through the length of the cavity

07 Accelerator Technology

T07 - Superconducting RF

in a region free of charge, a general complete solution to the fields can be found. The accelerating electric field can then be expressed as:

$$E_z(r,\phi,z) = E_z e^{i\omega t} = \sum_{n=0}^{\infty} r^n \left(E_z^{(n)} cos(n\phi) \right) e^{i\omega t}, \quad (1)$$

where E_z is the electric field along the beamline direction z and ω is the rf frequency. If the field $E_z(R,\phi,z)$ is known, then the coefficients $E_z^{(n)}$ can be found via inverse Fourier integration of the surface fitted field.

Using the Panofsky-Wenzel theorem we may then calculate the transverse change in momentum (kick) of the particles as a series of multipolar RF kicks:

$$\Delta p_\perp = \left(\frac{e}{\omega} \right) \int_{-\infty}^{+\infty} (-i)\nabla_\perp E_z|_{t=z/v_z} dz . \quad (2)$$

Finally, we can express the transverse rf-kicks in the notation commonly used for the multipole magnetic kick strength for magnets. It is important to notice that in our case, the transverse rf-kicks are not static, but functions of time, and as such, they are complex numbers oscillating at the rf-frequency of interest (400 MHz).

$$B^{(n)}(z) = \frac{nj}{\omega} E_z^{(n)}(z), \;\; b_n = \int_{-\infty}^{+\infty} B^{(n)}(z)dz . \quad (3)$$

Table 2 presents the multipolar components of the ideal cavity for reference. Because of the geometry of this cavity, all even b_n should be zero, so that gives us a reference for the degree of error in our calculations. Table 3 presents the multipole components for the cavities with the imperfections we have used as examples, namely for varying (A) yaw, (B) pitch, and (C) roll, normalized to $V_T = 1$ MV.

Table 2: RF Multipole Components, Normalized From Simulation Field Data to $V_T = 1$ MV, of the 400 MHz Rf-dipole Cavity

Multipole component		Units
V_T	1	MV
b_1	3.3	mT m
b_2	0.001	mT
b_3	37.4	mT/m
b_4	-1.8	mT/m^2
b_5	-1.94 x 10^5	mT/m^3

It can be seen that although higher order multipole components appear when the cavity is deformed, their contribution is not too significant (supported by the small percentage of variation in the transverse voltage profiles presented in the previous figures), and the cavity remains within the specifications required for the LHC crab cavity system.

Table 3: RF Multipole Components, Normalized From Simulation Field Data to $V_T = 1MV$, of the 400 MHz Rf-dipole Cavity. Units of mT m/m$^{(n-1)}$

Imperfection	b_1	b_2	b_3	b_4
yaw 1°	3.3	-0.003	36.1	41.1
yaw 2°	3.3	-0.0003	33.2	158.1
yaw 5°	3.3	-0.02	13.8	983.4
pitch 1°	3.3	-0.01	38.2	-18.1
pitch 2°	3.3	-0.05	40.4	-86.1
pitch 5°	3.3	-0.35	55.1	-561.4
roll 1°	3.3	-0.2	44.1	-171.0
roll 2°	3.3	-0.5	51.9	-374.6
roll 5°	3.3	-1.6	85.2	-1115.8

CONCLUSION

We are analyzing the impact of imperfections in the shape of the cavity on rf-parameters and multipole components. So far there are no deformations that would make the cavity non-compliant with the requirements for the LHC crab system. However, the analysis is not complete, and there can be significant shifts in the electrical center of the cavity. Our future plans include a comparison of these parameters for cavities normalized to the electrical center of the cavities, as opposed to normalization with respect to the ideal cavity.

REFERENCES

[1] S. U. De Silva and J. R. Delayen, "Design evolution and properties of superconducting parallel-bar rf-dipole deflecting and crabbing cavities," PRSTAB **16**, 012004 (2013).

[2] S. U. De Silva and J. R. Delayen, "Superconducting RF-Dipole Deflecting and Crabbing Cavities," SRF'13, Paris, France, September 2013, FRIOA04 (2013).

[3] Z. Li et al., "RF Modeling Using Parallel Codes ACE3P for the 400-MHz Parallel-Bar/Ridged-Waveguide Compact Crab Cavity for the LHC HiLumi Upgrade", IPAC'12 New Orleans, USA, May 2012, WEEPPB010 (2012).

[4] P. Baudrenghien, K. Brodzinski, R. Calaga, O. Capatina, E. Jensen, A. Macpherson, E. Montesinos, V. Parma, "Functional Specifications of the LHC Prototype Crab Cavity System", CERN-ACC-NOTE-2013-003 (2013).

[5] D. T. Abell, "Numerical computation of high-order transfer maps for rf cavities," PRSTAB **9**, 052001 (2006).

[6] J. Barranco Garcia et al., "Study of Multipolar RF Kicks from the main deflecting mode in compact crab cavities for LHC," IPAC'12, New Orleans, USA, May 2012, TUPPR027 (2012).

[7] R. G. Olave et al., "Multipole expansion of the fields in superconducting high-velocity spoke cavities" Proc. LINAC2012, Tel-Aviv Israel, MOPB072 (2012).

[8] S. U. De Silva and J. R. Delayen, "Multipole field effects for the superconducting parallel-bar/rf-dipole deflecting/crabbing cavities" Proc. LINAC2012, Tel-Aviv Israel, SUPB038 (2012).

07 Accelerator Technology

T07 - Superconducting RF